Analysis of Reflectance and Transmittance Measurements on Absorbing and Scattering Small Samples Using a Modified Integrating Sphere Setup

Jernshøj, Kit Drescher; Hassing, Søren

Published in:
Applied Spectroscopy

Publication date:
2009

Document Version
Final published version

Analysis of Reflectance and Transmittance Measurements on Absorbing and Scattering Small Samples Using a Modified Integrating Sphere Setup

K. D. JERNSHØJ and S. HASSING*

Institute of Sensors, Signals and Electrotechnics (SENSE), The Technical Faculty, University of Southern Denmark, Campusvej 55, DK-5230 Odense M, Denmark

The aim of the present paper is to analyze reflectance and transmittance measurements on small scattering and absorbing samples. The long term goal is to perform quantitative, spectroscopic *in vivo* measurements of pigments in small samples of plant material. Small samples such as small leaves constitute a special experimental challenge in cases in which the sample beam has a larger cross-sectional area than the sample. The experimental errors introduced when measuring reflectance and transmittance on small absorbing and scattering samples are investigated theoretically and experimentally by using a blue polyester sample as an appropriate test sample. The experiments are performed with either a mask or a lens setup combined with a mask inserted in the sample beam. In particular, the errors introduced in the reflectance measurements can be very large and larger than 100%. It is shown that any direct illumination of the mask must be avoided. To obtain more accurate values for the reflection coefficient it is necessary to combine the mask with a focusing lens system, adjust the mask and sample very carefully, and choose the ratio between the aperture of the mask and the beam area as large as possible. In the case of transmittance measurements, it is shown that the combination of a special sample fixture and a lens system gives rise to smaller errors compared to the errors introduced by the mask alone or the mask combined with a focusing lens system.

Index Headings: **Small samples; Masking; Lens system; Spectrophotometer; Reflectance; Transmittance; Transmission; Reflection.**

INTRODUCTION

Reflection spectroscopy is being applied increasingly in a vast number of fields because of the possibility of carrying out nondestructive measurements on various types of samples. One of the fields of application is the ability to assess a pigment content nondestructively, which is most valuable in terms of acquiring knowledge about or monitoring the physiological status of a plant. Using reflection spectroscopy enables nondestructive access to this information as opposed to the very tidy process of determining the content destructively by using absorption spectroscopy on the extracted and dissolved pigment. The applicability of reflection spectroscopy to the determination of the pigment content in different parts of the plants requires, however, that highly accurate and reproducible measurements can be made. An investigation and discussion of how to obtain such measurements is the main focus of this paper. The sample is represented by a test sample, a piece of blue polyester.

The reflectance and transmittance measurements are typically carried out using a conventional spectrophotometer equipped with an integrating sphere to collect the scattered radiation. A problem arises, however, when the measurements are performed on smaller samples, such as sepals and bracts, or when high spatial resolution is required. The smaller samples constitute a special experimental challenge, simply because they are too small to physically fit into the standard aperture or port of an integrating sphere. This requires the use of a mask to hold the sample in place, thereby reducing the aperture of the sample and entrance port. Also, the mask must ensure that a high degree of reproducibility is preserved. Since the beam provided by a standard spectrophotometer often has a larger cross-sectional area than the size of a small sample, it causes a direct illumination of the mask.

The impediments that result from measurements that are performed using a mask to reduce the aperture size will later be illustrated by the derived equations for evaluation of experimental data provided by the instrument. The equations reveal contributions caused by the direct illumination of the mask, but more interestingly, they also reveal interactions between the mask, the sample, and the port due to multiple scattering effects. Since these interactions depend on both the particular sample under investigation and on the wavelength, it is not possible to make simple corrections to eliminate this effect. The derived equations cover the case in which the sample beam is masked at the sample port (reflectance measurements) as well as the case in which the beam is masked at the entrance port (transmittance measurements).

Next, different approaches for measuring reflectance and transmittance from the previously mentioned small samples have been investigated, which most importantly provides more accurate results. In addition to using the mask in reflectance measurements and a pair of thin but rigid supports in transmittance measurements, a lens setup is placed in the beam path to reduce the size of the beam spot to less than the size of the mask. In this way the different contributions from the mask and the interactions among the mask, the sample, and the port are minimized. In principle, diffraction effects might occur, but in our opinion the deviations introduced from these effects are minor compared to the other mentioned effects that cause deviations. Diffraction effects will therefore be neglected in this article.

A lens setup has been designed that can easily be removed from the spectrophotometer such that the original design of the spectrophotometer has not been changed. As will be shown later, the settings of the instrument are very important in cases in which changes in the sphere (mask and/or mask combined with focusing optics) are made.

REFLECTION AND TRANSMISSION SPECTROSCOPY

The spectrophotometer used to perform the measurements appearing in this paper is a double-beam spectrometer of the

Received 12 February 2009; accepted 7 May 2009.
* Author to whom correspondence should be sent. E-mail: sh@sense.sdu.dk.

0003-7028/09/6308-0879$2.00/0

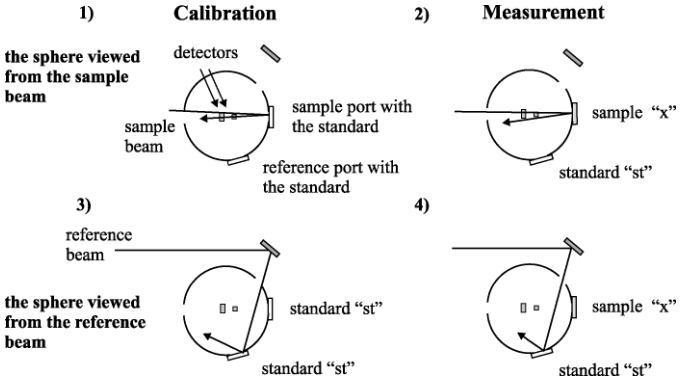

FIG. 1. The integrating sphere in two situations, i.e., in the measuring of the baseline and in the actual reflectance measuring situation.

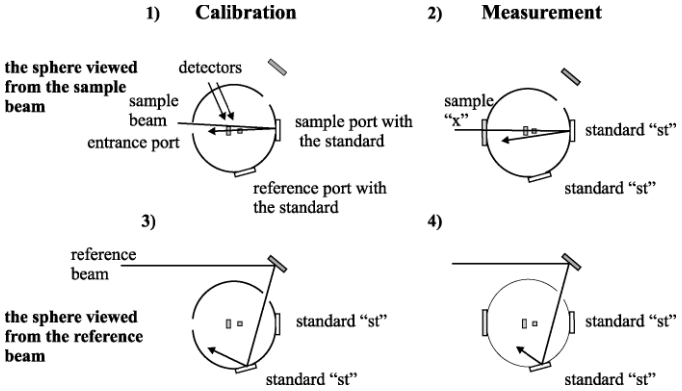

FIG. 2. The integrating sphere in two situations, i.e., in the measuring of the baseline and in the actual transmittance measuring situation.

type Perkin Elmer, Lambda 900 with a Labsphere integrating sphere option. The integrating sphere, which is 150 mm in diameter, is equipped with 25 mm port apertures. The spectrophotometer covers the wavelength range 185–3300 nm. In the ultraviolet and visible range the signal is detected by a photomultiplier and in the near-infrared range by a lead sulfide (PbS) detector.

To be able to address the different phenomena arising when applying a mask in the setup, the expressions describing the conventional use of the spectrophotometer are set up first.

The basic principles, when using an integrating sphere and a double-beam spectrophotometer to perform reflectance and transmittance measurements, respectively, are sketched in Figs. 1 and 2. All measurements are carried out relative to a diffuse optical standard, Spectralon®, which is a white thermoplastic resin with diffuse reflectance values between 95–99% in the wavelength region from 250 nm to 2500 nm. The samples, which in our case primarily are different kinds of leaves, have earlier been investigated and found to be absorbing and diffusively scattering. In this paper, however, measurements on a blue polyester material are used as the basis for the discussion of reflectance and transmittance measurements. The blue polyester, denoted from now on as the test sample, is characterized as a diffuse scatterer with high absorption in the visible spectral region. The test sample is made of homogeneously wound fibers with a diameter of approximately 300 μm. The scattering and absorption stems from the weave structure and cloth yarn structure of the test sample and is basically determined by the optical properties of the yarn. The scattering and absorption originates from the surface of the structure and from deeper within the structure. A physical model of the scattering properties of a similar sample is analyzed in Ref. 7.

The nomenclature used in the following is specified below:

(1) E_s and E_r are the energy of the sample and reference beam, respectively, just outside the integrating sphere.
(2) $\rho^{(i)}$ is the reflectance of the objects placed in the ports, where $i = st$, x, and m, which refer to the standard (Spectralon®), the sample, and the mask, respectively.
(3) Two parameters for reflectance and two parameters for transmittance measurements are needed to describe the effectiveness with which the energy reflected from an object will be captured by the integrating sphere and converted to a signal by the detector. The value of the parameters depends on the internal structure of the sphere, including the ports and the optical properties of the objects placed in the ports. In particular, when a mask is used, the thickness, the aperture, and the material (expressed by the reflectance, $\rho^{(m)}$) of the mask have a large effect on the parameters. Each parameter will be specified by a subscript r or s referring to the reference or the sample port/entrance port of the sphere.

In the case of reflectance measurements they will be specified by two superscripts, while in the case of transmittance measurements, three superscripts are required. The two parameters referring to reflectance measurements are: $k_s^{(i,st)}$ and $k_r^{(st,i)}$ where $i = x$, st, m, $x + m$, and $st + m$ and, e.g., $i = x + m$ means that both the mask and the object in question are placed in the port. The two parameters referring to transmittance measurements are: $k_s^{(st,st,i)}$ and $k_r^{(st,st,i)}$, where $i = x$, m, and $x + m$.

With respect to reflectance measurements, the first variable refers to the type of object placed in the directly illuminated port and the second variable refers to the type of object placed in the indirectly illuminated port, i.e., the port illuminated only by the light reflected from the surface of the integrating sphere. In the case of transmittance measurements, the last two variables refer to the type of objects placed in the indirectly illuminated ports. It should be noted that the value of the parameters does not only depend on the type of objects placed in the directly illuminated ports, but also on the objects placed in the indirectly illuminated ports as indicated by the nomenclature.

Review of Unmasked Measurements. The value B_R, recorded during an unmasked baseline correction in reflectance measurements, is described by Eq. 1:

$$B_R = \frac{E_s \cdot \rho^{(st)} \cdot k_s^{(st,st)}}{E_r \cdot \rho^{(st)} \cdot k_r^{(st,st)}} \tag{1}$$

During measuring the following value is recorded, S_R:

$$S_R = \frac{E_s \cdot \rho^{(x)} \cdot k_s^{(x,st)}}{E_r \cdot \rho^{(st)} \cdot k_r^{(st,x)}} \tag{2}$$

The reflectance value shown on the computer, $D_R^{(x)}$, is, however, represented by Eq. 3, which is the ratio between

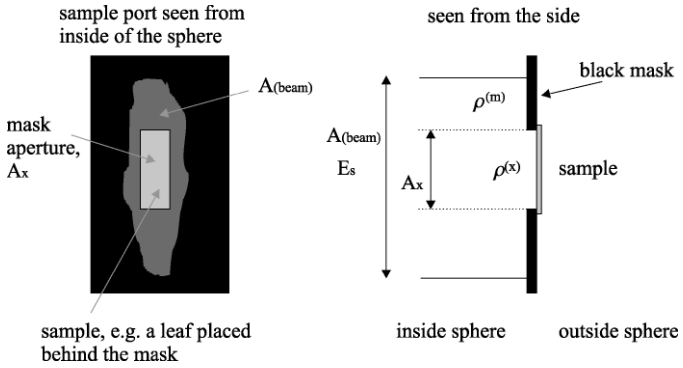

FIG. 3. The geometry and the nomenclature used in later equations describing reflectance measurements. The area of the mask aperture is approximately 2×6 mm^2 and the area of the beam in the sample port is approximately 3×13 mm^2.

Eqs. 1 and 2:

$$D_R^{(x)} = \frac{\rho^{(x)}}{\rho^{(st)}} \cdot \frac{k_s^{(x,st)}}{k_r^{(st,x)}} \tag{3}$$

Due to symmetry it has been assumed that $k_s^{(st,st)} \approx k_r^{(st,st)}$. The true reflectance of the sample must be calculated using Eq. 4:

$$\rho^{(x)} = D_R^{(x)} \cdot \rho^{(st)} \cdot \frac{k_r^{(st,x)}}{k_s^{(x,st)}} \tag{4}$$

which may be reduced to Eq. 5 when $k_r^{(st,x)} \approx k_s^{(x,st)}$. This reduction requires that the surface structure of the sample does not differ too much from the surface structure of the standard used. Besides, depending on the inner structure of the sample, wavelength-dependent multiple scattering may cause deviations from the simple result given in Eq. 5:

$$\rho^{(x)} = D_R^{(x)} \cdot \rho^{(st)} \tag{5}$$

This expression is typically used in standard reflectance measurements.[4] The baseline correction B_T, recorded when measuring transmittance, is given by Eq. 6:

$$B_T = \frac{E_s \cdot \rho^{(st)} \cdot k_s^{(st,st)}}{E_r \cdot \rho^{(st)} \cdot k_r^{(st,st)}} \tag{6}$$

The following expression describes the value recorded during measurements:

$$S_T = \frac{T_x \cdot E_s \cdot \rho^{(st)} \cdot k_s^{(st,st,x)}}{E_r \cdot \rho^{(st)} \cdot k_r^{(st,st,x)}} \tag{7}$$

The value shown on the computer is scaled with the value recorded during the baseline correction as follows:

$$D_T^{(x)} = \frac{S_T}{B_T} = \frac{T_x \cdot E_s \cdot \rho^{(st)} \cdot k_s^{(st,st,x)}}{E_r \cdot \rho^{(st)} \cdot k_r^{(st,st,x)}} \cdot \frac{E_r \cdot \rho^{(st)} \cdot k_r^{(st,st)}}{E_s \cdot \rho^{(st)} \cdot k_s^{(st,st)}} = T_x \cdot \frac{k_s^{(st,st,x)}}{k_r^{(st,st,x)}} \tag{8}$$

$$T_x = D_T^{(x)} \cdot \frac{k_r^{(st,st,x)}}{k_s^{(st,st,x)}} \tag{9}$$

Equation 9 may be reduced to Eq. 10:

$$T_x = D_T^{(x)} \tag{10}$$

when $k_s^{(st,st,x)} \approx k_r^{(st,st,x)}$. This requires, however, that scattering in the transmitting sample is negligible. Equation 10 is typically used in standard transmittance measurements. If the sample is highly scattering, deviations from Eq. 10 must be expected.[4]

Analysis of Masked Measurements. Equations for evaluation of the experimental data provided by the instrument are derived for two cases, **1**, in which the sample beam is masked at the sample port (reflectance measurements), and **2**, in which the sample beam is masked at the entrance port (transmittance measurements).

In general the mask should be designed in such a way that the influence on the measurements is minimized. Therefore, several demands are to be imposed on the physical layout of the mask, including the choice of material, color, and thickness. The mask is normally painted a diffusive black in order to reduce contributions from the mask itself.[3] The effect of the thickness of the mask has been analyzed by A. Brunsting et al.[1] Ideally the mask should be infinitely thin but rigid enough to locate reproducibly all potential sample surfaces.

In the following subsection the equations describing masked reflectance measurements are derived.

Analysis of Masked Reflectance Measurements. Figure 3 illustrates the different areas and the nomenclature used in the equations describing the reflectance measurements. When the mask is used, Eqs. 1, 2, 3, and 4, presented above, are modified as follows:

$$B_{R,m} = \frac{\left(E_s/A_{(beam)}\right) \cdot \left[A_x \cdot \rho^{(st)} + \left(A_{(beam)} - A_x\right) \cdot \rho^{(m)}\right] \cdot k_s^{(st+m,st)}}{E_r \cdot \rho^{(st)} \cdot k_r^{(st,st+m)}} \tag{11}$$

$$S_{R,m} = \frac{\left(E_s/A_{(beam)}\right) \cdot \left[A_x \cdot \rho^{(x)} + \left(A_{(beam)} - A_x\right) \cdot \rho^{(m)}\right] \cdot k_s^{(x+m,st)}}{E_r \cdot \rho^{(st)} \cdot k_r^{(st,x+m)}} \tag{12}$$

$$D_{R,m}^{(x)} = \frac{S_{R,m}}{B_{R,m}} = \frac{\rho^{(x)} + a_R \rho^{(m)}}{\rho^{(st)} + a_R \rho^{(m)}} \cdot \frac{k_s^{(x+m,st)} \cdot k_r^{(st,st+m)}}{k_s^{(st+m,st)} \cdot k_r^{(st,x+m)}} \tag{13}$$

where a_R is defined as $a_R = (A_{(beam)} - A_x)/A_x$. In Eqs. 11, 12, and 13 it has been assumed that the sample beam has a homogeneous intensity distribution. When this is not the case, an integration over the beam area must be performed; this, however, does not change the general result.

The true reflectance of the sample is now given as:

$$\rho^{(x)} = D_{R,m}^{(x)} \cdot \rho^{(st)} \cdot \frac{k_s^{(st+m,st)} k_r^{(st,x+m)}}{k_s^{(x+m,st)} k_r^{(st,st+m)}} + D_{R,m}^{(x)} \cdot a_R \rho^{(m)} \cdot \frac{k_s^{(st+m,st)} k_r^{(st,x+m)}}{k_s^{(x+m,st)} k_r^{(st,st+m)}} - a_R \rho^{(m)} \tag{14}$$

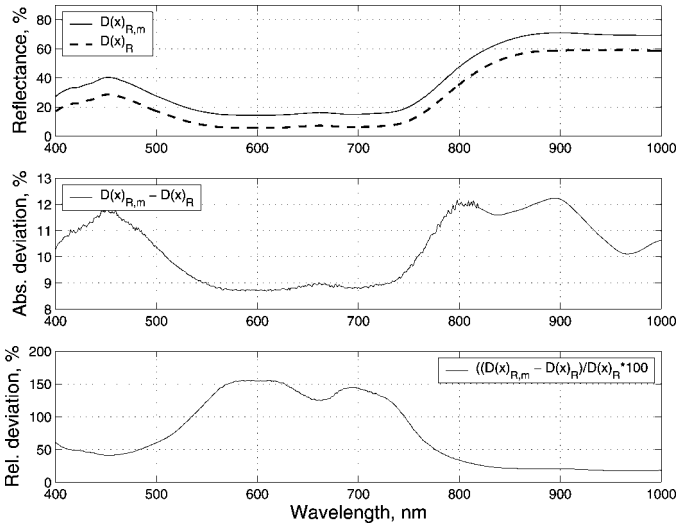

FIG. 4. The reflectance spectra of the test sample, which are obtained with $D_{R,m}^{(x)}$ and without $D_R^{(x)}$ a black mask. The calculated absolute and relative deviations are also shown.

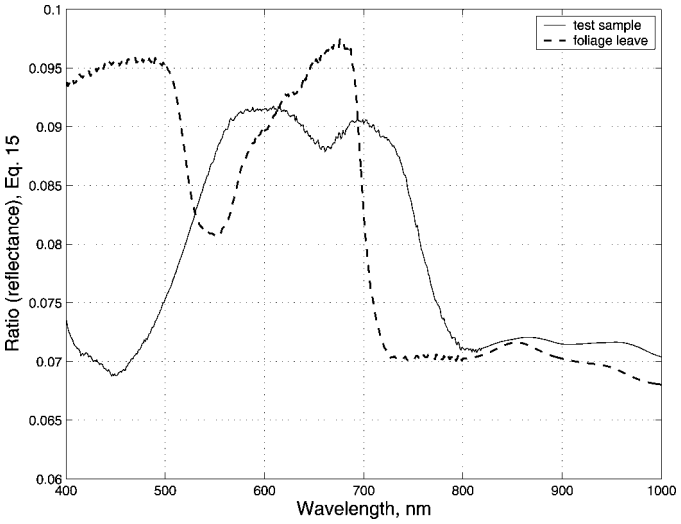

FIG. 5. The ratio of the k-parameters (reflectance) given by Eq. 15 in which the test sample and hibiscus foliage leaf data are inserted.

When Eq. 14 is compared to Eq. 4, it is seen that due to the mask, the expression describing the reflectance of the sample contains three terms instead of just one as in Eq. 4.

The first term in Eq. 14 corresponds to the term in Eq. 4, except that the output from the instrument $D_{R,m}^{(x)}$ is multiplied by a factor containing four parameters. In the second term, $D_{R,m}^{(x)}$ is again multiplied by the factor containing the four parameters and by the product of the reflectivity of the mask material and a_R, which describes the relative size of the mask. If the mask is considered a perfect blackbody, Eq. 14 is reduced to Eq. 4. The third term is just the product of the reflectivity of the mask material and a_R. Although the third term may be large, it can easily be corrected for, since the size and the reflectivity of the mask can be determined. The real challenge is the appearance of the four parameters discussed above.

As already stated, the parameters reflect the combined effect of various phenomena taking place in the sphere during the measurements. Since the parameters depend on the optical properties of the objects (i.e., sample, mask, and standard) placed in the ports, it is in general not possible to find an accurate correction of the output from the instrument. The main cause of this is the interplay between the mask and the inner structure of the sample and also in particular the size of this structure in comparison with the analyzing wavelength. This interplay may give rise to multiple scattering, which again in combination with the mask results in an increased diffuse reflection.

The error introduced is clearly illustrated by the reflectance measurements performed on the test sample. These reflectance measurements, performed with a mask $D_{R,m}^{(x)}$ and without a mask $D_R^{(x)}$, are shown in Fig. 4, together with the absolute and relative deviations.

Postprocessing of all raw data has been applied in the wavelength region 800–1000 nm in order to be able to make a reliable evaluation of the experimental improvements introduced later. The postprocessing consists of a combination of a fast Fourier transform (FFT) analysis and a wavelet based smoothing. From Fig. 4 it follows that a higher reflectance, around 10%, is obtained in the whole wavelength region when the mask is used. The variation in the absolute deviation lies within 4%. When the relative error is considered, however, it is seen that the introduction of the mask gives rise to very large errors, in particular in the visible region of 550 to 750 nm, where the relative error is around 150%. In this region both the reflectance and the transmittance values (see Figs. 4 and 7) are very low, which shows that the sample is strongly absorbing in this region. Since the scattering from the sample itself is small, the various scattering phenomena involving the mask are therefore more readily observed in this region than in the regions where the scattering from the sample is larger. The results shown in Fig. 4 also have the consequence that reflectance values below approximately 20% become highly inaccurate when a mask is used to reduce the beam area.

One way of illustrating the errors introduced by the mask is to estimate the ratio of the k-parameters. This ratio can be estimated by writing Eq. 14 as follows:

$$\frac{k_s^{(st+m,st)} \cdot k_r^{(st,x+m)}}{k_s^{(x+m,st)} \cdot k_r^{(st,st+m)}} \simeq \frac{D_R^{(x)} + a_R D_R^{(m)}}{D_{R,m}^{(x)} \cdot \left(1 + a_R D_R^{(m)}\right)} \qquad (15)$$

where we have inserted the approximation given by Eq. 5 for $\rho^{(x)}$ and $\rho^{(m)}$. Notice again, that if the mask acts as a perfect blackbody, the ratios shown in Eq. 15 are equal to one.

To determine the ratio in Eq. 15 experimentally, the reflectance spectra of the test sample with the use of a black mask, $D_{R,m}^{(x)}$, and without the use of the mask, $D_R^{(x)}$, have been inserted together with the reflectance spectrum of the mask material.

The mask used in the measurements is made of 0.19 mm thick brass foil, which is painted a matte black as recommended in Ref. 3. Since the aim is to obtain reflectance spectra of the bracts of hibiscus and plant material of similar size, the aperture of the mask is chosen so that the bracts just fill the aperture. The aperture of the mask is therefore rectangular with dimensions of 2×6 mm^2. The size of the beam in the reflection sample port is approximately 3×13 mm^2 and in the sample port is approximately 8×13 mm^2.

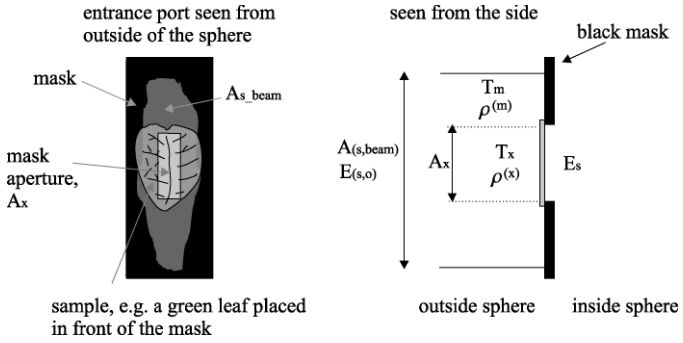

FIG. 6. The geometry and nomenclature that are used in the equations describing transmittance measurements. The area of the mask aperture is approximately 2×6 mm^2 and the beam area in the entrance port (see Fig. 2) is approximately 8×13 mm^2.

Figure 5 shows the ratio of the parameters obtained by inserting the test sample data in Eq. 15. For a comparison, data obtained from a Hibiscus foliage leaf has also been inserted in Eq. 15. This figure shows that the ratio of the parameters deviates strongly from one when the mask is introduced and that the ratio depends on the wavelength. It should be noticed that this wavelength dependence is connected with the properties of the sample, and therefore it is not possible to find a general and accurate way to correct the reflectance data when the mask is used. As an attempt to improve the accuracy of the measurements performed with a mask, measurements with no sample but a beam dump in its place have been recorded. Ideally this should give a reflectance value equal to zero; instead, a constant value was obtained, which should be subtracted from the reflectance measurements performed with only the mask.

Analysis of Masked Transmittance Measurements. Figure 6 illustrates the different areas and the nomenclature that are used in the equations describing the transmittance measurements. The measuring situation is analyzed in two different cases, namely:

(1) when the sample is just filling the aperture of the mask, i.e., $A_m \simeq A_x$, and
(2) when the sample is larger than the mask aperture and therefore covering the mask, i.e., $A_x > A_{beam} > A_m$.

If $T_m = 0$, it is seen that case 2 is equal to case 1.
The baseline correction $B_{(T,m)}$ is given by Eq. 16:

$$B_{T,m} = \left\{ \left(E_{(s,beam)}/A_{(beam)} \right) \times \left[A_x \cdot 1 + \left(A_{(beam)} - A_x \right) \cdot T_m \cdot \rho^{(st)} \cdot k_s^{(st,st,m)} \right] \right\} \div \left[E_r \cdot \rho^{(st)} \cdot k_r^{(st,st,m)} \right] \quad (16)$$

The following expression describes the value recorded during measurement:

$$S_{T,m} = \left\{ \left(E_s/A_{(s,beam)} \right) \cdot \left[A_x \cdot T_x + \left(A_{(s,beam)} - A_x \right) \cdot T_m \right] \times \rho^{(st)} \cdot k_s^{(st,st,x+m)} \right\} \div \left[E_r \cdot \rho^{(st)} \cdot k_r^{(st,st,x+m)} \right] \quad (17)$$

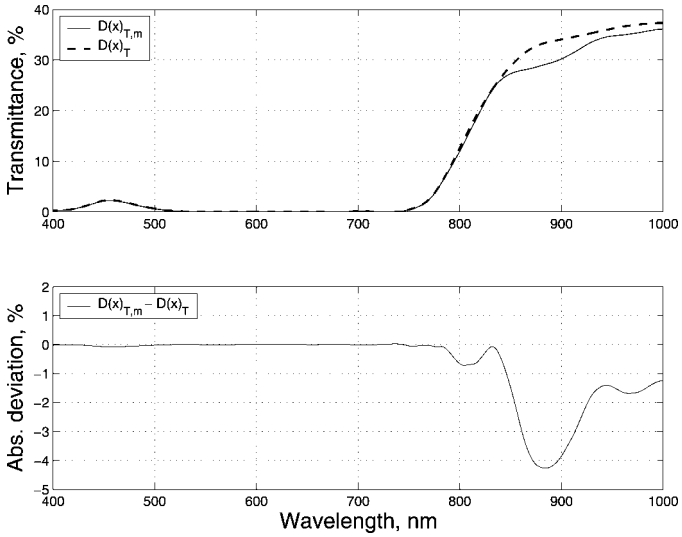

FIG. 7. The transmittance spectra of the test sample. These are obtained with $D_{T,m}^{(x)}$ and without $D_T^{(x)}$ a black mask. The calculated absolute deviation is also shown.

The transmittance value shown on the computer is represented by Eq. 18:

$$D_{T,m}^{(x)} = \frac{S_{T,m}}{B_{T,m}} = \frac{A_x \cdot T_x + \left(A_{(s,beam)} - A_x \right) \cdot T_m}{A_x + \left(A_{(s,beam)} - A_x \right) \cdot T_m} \cdot \frac{k_s^{(st,st,x+m)}}{k_r^{(st,st,x+m)}} \cdot \frac{k_r^{(st,st,m)}}{k_s^{(st,st,m)}} = \left(\frac{T_x + a_T \cdot T_m}{1 + a_T \cdot T_m} \right) \cdot \frac{k_s^{(st,st,x+m)}}{k_r^{(st,st,x+m)}} \cdot \frac{k_r^{(st,st,m)}}{k_s^{(st,st,m)}} \quad (18)$$

where a_T is defined as $a_T = (A_{(s,beam)} - A_x)/A_x$.

Equation 18 is then rearranged to give the actual equation describing the transmittance in case **1**:

$$T_x = D_{T,m}^{(x)} \cdot (1 + a_T \cdot T_m) \cdot \frac{k_r^{(st,st,x+m)}}{k_s^{(st,st,x+m)}} \cdot \frac{k_s^{(st,st,m)}}{k_r^{(st,st,m)}} - a_T \cdot T_m = D_{T,m}^{(x)} \cdot \frac{k_r^{(st,st,x+m)}}{k_s^{(st,st,x+m)}} \cdot \frac{k_s^{(st,st,m)}}{k_r^{(st,st,m)}} + a_T \cdot T_m \cdot \frac{k_r^{(st,st,x+m)}}{k_s^{(st,st,x+m)}} \cdot \frac{k_s^{(st,st,m)}}{k_r^{(st,st,m)}} - a_T \cdot T_m \quad (19)$$

When Eq. 20 is compared to the expression given in Eq. 9, which describes the transmittance obtained without the use of a mask, it follows that Eq. 20 is generally modified in a similar way as in the case of reflectance, i.e., when Eq. 14 is compared to Eq. 4.

However, as seen from a comparison between Eq. 20 and Eq. 14, the parameters related to transmittance will differ from the parameters related to reflectance. Three indices are needed to specify the parameters in the equation relating to transmittance since changes are now made to the entrance port as well.

If the sample is covering the mask (case **2**), Eqs. 18 and 20 must be changed accordingly:

$$D_{T,m}^{(x)} = \left[\frac{T_x \cdot (1 + a_T \cdot T_m)}{1 + a_T \cdot T_m \cdot T_x} \right] \cdot \frac{k_s^{(st,st,x+m)}}{k_r^{(st,st,x+m)}} \cdot \frac{k_r^{(st,st,m)}}{k_s^{(st,st,m)}} \quad (20)$$

and

$$T_x = \frac{D_{T,m}^{(x)}}{\frac{k_s^{(st,st,x+m)}}{k_r^{(st,st,x+m)}} \cdot \frac{k_r^{(st,st,m)}}{k_s^{(st,st,m)}} \cdot \left(1 + a_T \cdot D_T^{(x)} T_m\right) - D_{T,m}^{(x)} \cdot a_T \cdot T_m} \tag{21}$$

Transmittance spectra of the test sample have been recorded with the mask placed in the entrance port, $D_{T,m}^{(x)}$, and without a mask, $D_T^{(x)}$. The mask used here is the same mask as was used in the reflectance measurements. The spectra are shown in Fig. 7 together with the absolute and relative deviations.

As opposed to the reflectance measurements, the errors introduced in the transmittance measurements are much smaller. This is due to the nature of the transmittance measurements. Since the transmittance of the mask is very low, only a small amount of the light illuminating the mask will enter the sphere.

It follows from Fig. 7 that the accuracy of the transmittance measurements of the test sample is quite good. The relative deviations at 880 nm are approximately 15%. The obtainable accuracy will in general depend on the inner structure of the sample. The test sample is made of homogeneously wound fibers, with a diameter of approximately 300 μm. This signifies that the angular distribution of the scattering from different sample points is the same. The inner structure of the leaves, however, is not homogeneous and will vary for different kinds of leaves.

The influence of the *k*-parameters on the transmittance can be estimated from Eqs. 18 to 20 as follows.

In case **1** the equation is derived by applying the conditions specified in Eqs. 10 to 20:

$$\frac{k_s^{(st,st,x+m)}}{k_r^{(st,st,x+m)}} \cdot \frac{k_r^{(st,st,m)}}{k_s^{(st,st,m)}} = D_{T,m}^{(x)} \cdot \frac{1 + a_T \cdot D_T^{(m)}}{D_T^{(x)}} + a_T \cdot D_T^{(m)} \tag{22}$$

In case **2** the equation is derived by applying the conditions specified in Eqs. 10 to 20:

$$\frac{k_s^{(st,st,x+m)}}{k_r^{(st,st,x+m)}} \cdot \frac{k_r^{(st,st,m)}}{k_s^{(st,st,m)}} = D_{T,m}^{(x)} \cdot \frac{1 + a_T \cdot D_T^{(m)} \cdot D_T^{(x)}}{D_T^{(x)} \cdot \left(1 + a_T \cdot D_T^{(m)}\right)} \tag{23}$$

The test sample data are used in order to evaluate Eq. 23. The transmittance of the mask has been measured with the result that it is close to zero at all wavelengths from 400 to 1000 nm. The ratio determined from Eq. 23 with $D_T^{(m)} \simeq 0$ and $[k_s^{(st,st,x+m)}/k_r^{(st,st,x+m)}] \cdot [k_r^{(st,st,m)}/k_s^{(st,st,m)}] \simeq [D_{T,m}^{(x)}/D_T^{(x)}]$ is depicted in Fig. 8. From approximately 540 to 740 nm, the transmittance values are zero; the ratio has therefore been omitted in this range. It follows from the figure that accurate transmittance measurements on homogeneous samples can be made with the usage of a properly chosen mask. The mask, in combination with an inhomogeneous sample, might, as mentioned above, introduce wavelength-dependent scattering phenomena, which it is not possible to correct for.

SPECTROPHOTOMETRY APPLIED TO SMALL SAMPLES

The next section is initiated by introducing a measuring method usable for reflectance measurements, which is based on the usage of a mask and a lens setup. By introducing a lens setup, the mask will no longer be directly illuminated and the contribution from the mask is nearly eliminated.

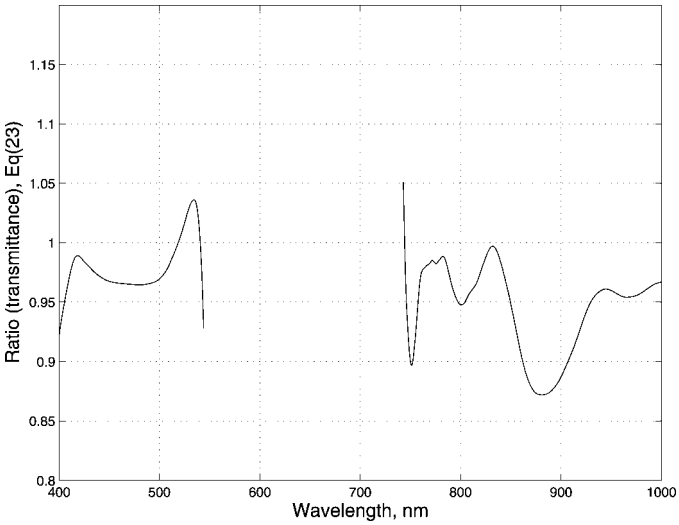

FIG. 8. The *k*-ratio given by Eq. 23. The calculation is done with the test sample data. From approximately 540 to 740 nm, the transmittance values are zero; the ratio has been omitted in this range.

Next, the transmittance measurements are carried out using the same measuring principle as stated above. Besides this, measurements obtained without the use of a mask but the sample freely suspended in the entrance port will be carried out and compared to the formerly mentioned measurements.

In the case of transmittance measurements, the advantages and disadvantages of using either a mask or a beam condenser have been listed in Ref. 5. According to Ref. 5, the main disadvantage of using a mask to reduce the sample beam is that the signal-to-noise ratio in these measurements will be lower compared to the measuring done with the unmodified beam. A careful analysis of the effect of introducing a mask in the case of reflectance and transmittance is, however, not presented in Refs. 3–6. Besides, to our best knowledge, it is not possible to find such an analysis elsewhere. The analysis carried out in the present paper clearly shows that the reduction of the signal-to-noise ratio is in most cases not important for either reflectance or transmittance measurements. The main problem is that the mask gives rise to wavelength and sample-dependent scattering phenomena. The interplay between the directly illuminated mask and the sample may cause large measuring errors. In general, the magnitude of these errors will be much larger in reflectance than in transmittance measurements.

The cross-section of the beam can be altered in different ways inside the spectrometer, thereby eliminating the different contributions from the mask caused by direct illumination of the mask.

In Ref. 1, serious modifications of a particular spectrometer are described. The modifications proposed in Ref. 1 are not applicable in general, since the optics are not accessible in most commercial instruments. In the following, one alteration is explored, i.e., the cross-section of the sample beam is reduced by inserting a removable optical system into the sample beam. The cross-section is thus reduced to a size primarily determined by the smaller aperture of the mask and is furthermore focused onto the sample. In this way it is not necessary to modify any optics preinstalled from the factory.

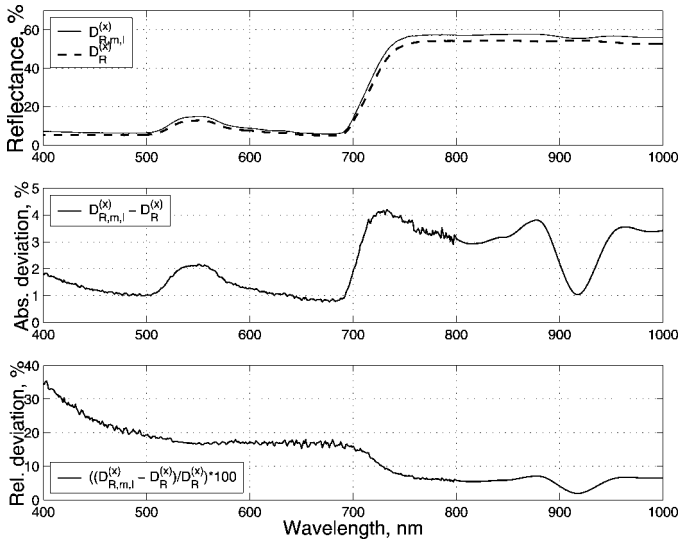

FIG. 9. The reflectance spectra of the test material, which are obtained in the following ways: (1) with the modified setup comprising a lens setup and the mask, $D^{(x)}_{R,m,l}$, and (2) with the conventional setup, without modifications or use of a mask, $D^{(x)}_R$. The calculated absolute and relative deviations between (1) and (2) are also shown.

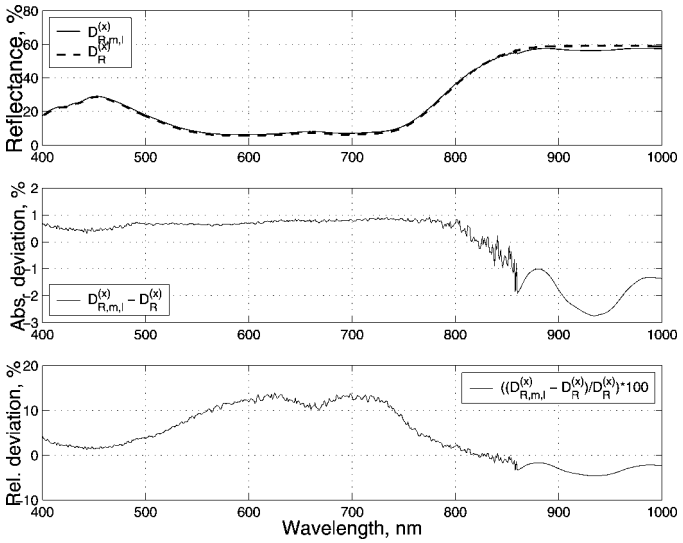

FIG. 10. The reflectance spectra of the test sample, where the ratio between the aperture of the mask and the beam area has been increased by a factor of 4. The reflectance spectra are obtained in the following ways: (1) with the modified setup comprising a lens setup and the mask, $D^{(x)}_{R,m,l}$, and (2) with the conventional setup, without modifications or use of a mask, $D^{(x)}_R$. The calculated absolute and relative deviations between (1) and (2) are also shown.

Two different lens setups have been designed, one for usage in reflectance measurements and one for usage in transmittance measurements. When the beam area is reduced, the k-parameters are changed as well; therefore, Eqs. 14 and 20 must be considered once more.

In the case of reflectance measurements, the modified version of Eq. 14 becomes:

$$\rho^{(x)} = D^{(x)}_{R,m,l} \cdot \rho^{(st)} \cdot \frac{k_r^{(st,x+m)} \hat{k}_s^{(st+m,st)}}{\hat{k}_s^{(x+m,st)} k_r^{(st,st+m)}} \tag{24}$$

where $\hat{k}_s^{(x+m,st)}$ and $\hat{k}_s^{(st+m,st)}$ are the parameters modified due to the reduced beam area and $D^{(x)}_{R,m,l}$ is the reflectance spectrum obtained using the black mask together with the lens setup.

Using the approximation for $\rho^{(x)}$ given by Eq. 5, in Eq. 24, the modified version of Eq. 15 becomes:

$$\frac{\hat{k}_s^{(st+m,st)} \cdot k_r^{(st,x+m)}}{\hat{k}_s^{(x+m,st)} \cdot k_r^{(st,st+m)}} \simeq \frac{D^{(x)}_R}{D^{(x)}_{R,m,l}} \tag{25}$$

The reflectance spectrum $D^{(x)}_{R,m,l}$ of the test sample has been recorded and compared to the reflectance spectrum obtained without the mask and lens setup, $D^{(x)}_R$. The mentioned reflectance spectra are shown in Fig. 9 together with the absolute and relative deviations. Figure 9 reveals that the absolute deviation is now reduced to a variation between 1 and 4%. This variation is also wavelength dependent. The maximum relative deviation is reduced significantly from 150% to below 30%.

Two options are possible in order to investigate the error: (1) either the focusing lens system could be redesigned in order to obtain a smaller spot size, or (2) the mask aperture could be enlarged. In order to ensure that the affect from the mask has been completely eliminated, option 2 is chosen, in which the aperture of the mask is increased. The ratio between the mask aperture and beam area is chosen to be the same as the ratio between the sphere port aperture and the conventional beam area. The reflectance measurements carried out with this mask are shown in Fig. 10.

It follows from this figure that the errors introduced by the mask can be reduced by increasing the ratio between the aperture of the mask and the beam area. As seen, the maximum error has been reduced from 30% to 10%. It is, however, not possible to completely eliminate the error arising when a mask is used in the measurements. The wavelength-dependent interplay between the mask and the sample will still prevail. The reason for this is twofold, namely, (1) the mask aperture can not be made arbitrarily large, since it is determined by the size of the sample, and (2) the focused beam spot can not be made arbitrarily small.

To estimate the modified k-parameters from Eq. 25, the ratio between $D^{(x)}_R$ and $D^{(x)}_{R,m,l}$ has been calculated and is also depicted in Fig. 11. A comparison of this with the results calculated from Eq. 15 shows that the influence from the mask is strongly reduced by avoiding the direct illumination of the mask. The value of the ratio now lies between 0.8 and 0.9.

The results obtained in this section, regarding the reflectance of the test sample, are summarized in Fig. 12. As discussed previously, introducing the mask gives rise to a large error at all wavelengths; also, the error is strongly wavelength dependent. When the mask is combined with a focused sample beam so that the direct illumination of the mask is avoided, the measuring error is strongly reduced. The graph shown in Fig. 12 corresponds to a measurement in which the ratio between the mask aperture and the beam area is equal to 3, while in Fig. 10 this ratio is increased to 12. As mentioned above the error is then further reduced.

Notice that, the relative deviation obtained as a result of focusing is not exactly zero. This is due to the comparable size of the structure of the test sample and the beam area of the focused beam, which has the consequence that the experimental conditions are not completely the same as for the conventional beam, which is used as reference. The small

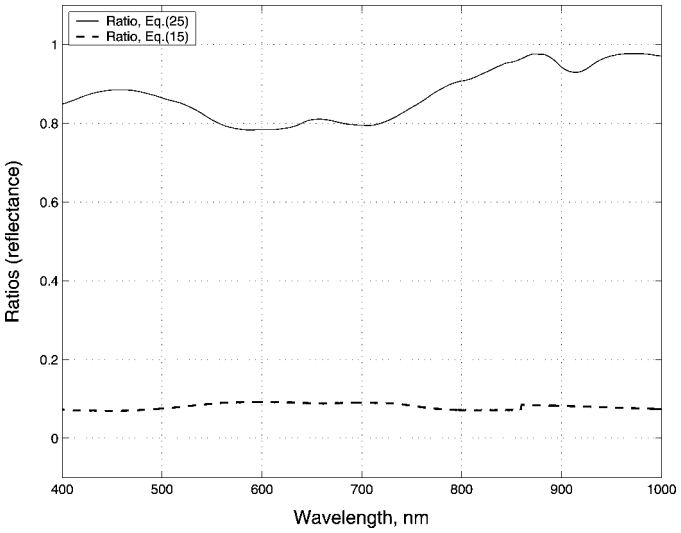

FIG. 11. The modified parameters have been estimated by calculating the ratio between $D_R^{(x)}$ and $D_{R,m,l}^{(x)}$ from Eq. 25. This ratio together with the ratio calculated from Eq. 15, which is obtained using only a mask, are shown.

relative deviation should therefore not be considered a measuring error.

Finally, it is possible due to the increased spatial resolution to illuminate selective areas of a large sample and determine the pigment concentration in these areas.

TRANSMITTANCE MEASUREMENTS USING A MASK/LENS SETUP OR A SUSPENSION OF THE SAMPLE/LENS SETUP

The final transmittance measurements described in this section are carried out using the previously discussed setup comprising a lens setup combined with either the mask or a suspension of the sample in the entrance port. The equations describing both measuring methods can be derived from the equations from the Analysis of Masked Transmittance

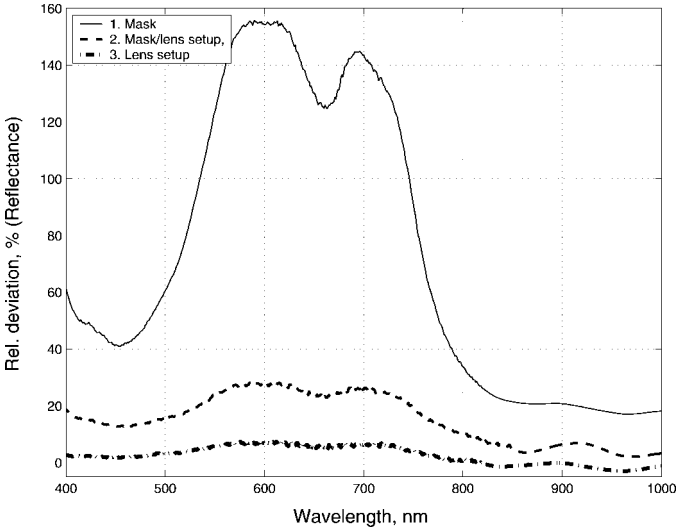

FIG. 12. The relative deviations between the conventional reflectance measurement and measurements using either (1) the mask, (2) the mask and lens setup, or finally, (3) only the lens setup are shown.

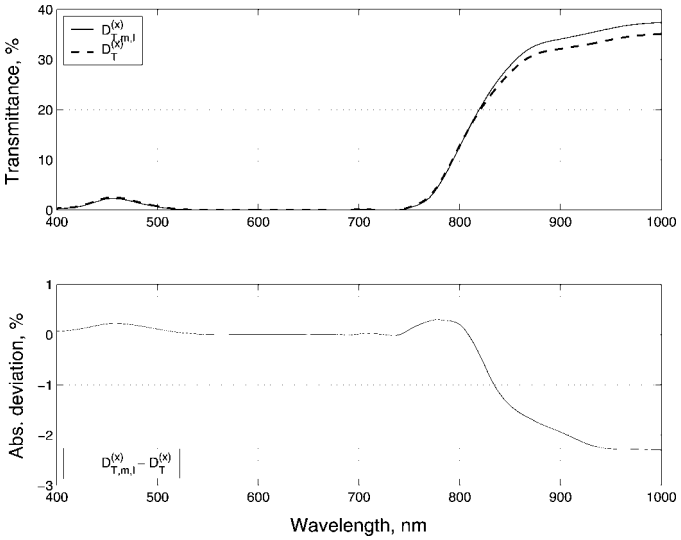

FIG. 13. The transmittance spectra of the test sample, which are obtained by using (1) the modified setup comprising a lens setup and the mask, $D_{T,m,l}^{(x)}$, and (2) the spectrometer without modifications or use of mask, $D_T^{(x)}$. The calculated absolute deviation between (1) and (2) is also shown.

Measurements section, described as case **1**:

$$T_x = D_{T,m,l}^{(x)} \cdot \frac{\hat{k}_s^{(st,st,x+m)}}{k_r^{(st,st,x+m)}} \cdot \frac{k_r^{(st,st,m)}}{\hat{k}_s^{(st,st,m)}} \tag{26}$$

$$\frac{\hat{k}_s^{(st,st,x+m)}}{k_r^{(st,st,x+m)}} \cdot \frac{k_r^{(st,st,m)}}{\hat{k}_s^{(st,st,m)}} \simeq \frac{D_T^{(x)}}{D_{T,m,l}^{(x)}} \tag{27}$$

The results of the measurements using the lens setup and mask are shown in Fig. 13. A comparison of Figs. 7 and 13 shows that the maximum relative error has been decreased from approximately 15% to 6%.

In order to optimize the setup for obtaining accurate values for the transmittance of small samples, the following measurements are considered. First, the transmittance of a small piece of the test sample is measured by attaching it to two thin rigid supports (see Fig. 14). The beam is not focused and the size of the test sample is slightly larger than the beam, which is 8×13 mm^2. The supports are not illuminated. This measuring setup renders the usage of the mask unnecessary since the sample is freely suspended in the entrance port. Due to the small area of the supports, the experimental conditions

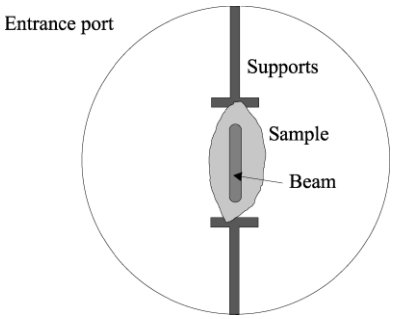

FIG. 14. A schematic drawing of the suspension used in the transmittance measurements.

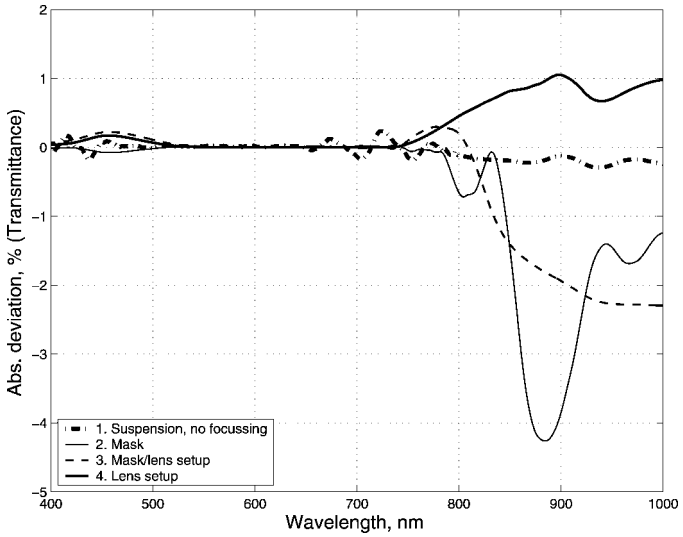

FIG. 15. The absolute deviations between the conventional transmittance measurement and the measurements using either (1) the mask, (2) the mask and lens setup, (3) only the lens setup, or finally, (4) suspension of the sample, but no focusing.

seen from the sphere are almost identical to the conditions in the conventional setup when the baseline correction B_T is recorded. In the measuring mode the only difference between the setup with the supports and the conventional setup is that in the conventional setup the sample is covering the whole aperture of the entrance port. However, for an optimized layout of the sphere this difference should not give rise to significant errors. The result of the transmittance obtained for the suspended small sample is shown in Fig. 15 together with the results obtained using (1) the mask, (2) the mask combined with the focusing lens setup, and (3) the focusing lens setup alone. The figure shows for each case the absolute deviation between the transmittance obtained with the conventional setup and the transmittance obtained for the four cases just mentioned. It follows from Fig. 15 that the absolute deviation between the conventional setup and the suspended sample (graph 4) is very small, as expected. It also follows that the mask gives rise to the largest deviation and that the mask combined with the focusing lens system improves the result. Finally, it is seen that the use of the focusing lens system alone apparently gives rise to a measuring error and that this gives rise to an increased transmittance. As mentioned in the discussion of the reflectance results, the experimental situation is changed when the beam is focused. This is due to the structure of the test sample. As concluded for the reflectance measurements, this should not be considered as a measuring error. On the other hand, it means that the transmittance measurement performed with the mask and lens is actually more accurate than shown in the figure.

It follows from the above that the most accurate transmittance measurement on a small sample is obtained by using the rigid supports to fix the sample, combined with a lens system with a focusing property determined by the size of the small sample.

As a concluding remark, the following should be considered. The use of lenses (BK7 glass) in the beam path imposes a few restrictions on the use of the spectrometer, specifically, a reduced usable range of wavelengths, approximately 350 to 1600 nm, as opposed to 185–3300 nm, when using the spectrometer without modifications. This restriction may be avoided by choosing a more appropriate lens material. Also, a small increase in reflection loss is to be expected, which eventually decreases the signal.

CONCLUSION

This paper has presented the theoretical and experimental considerations needed to improve the accuracy and reproducibility of the reflectance and transmittance measurements performed on small absorbing and scattering samples using an integrating sphere.

In the reflectance measurements, the sample beam was modified by using either a mask or a mask combined with focusing optics, the latter in order to avoid direct illumination of the mask. When the mask is used, a higher reflectance value is obtained in the whole wavelength region. When considering the relative error, it is found that the introduction of the mask gives rise to very large errors, in particular in the spectral region of 550 to 750 nm. It has been shown that when the mask is introduced in reflectance measurements, it is not possible to find a general and accurate way to correct the reflectance data, since the mask introduces wavelength- and sample-dependent deviations. When the beam is focused so that the direct illumination of the mask is avoided, the accuracy of the reflectance is increased considerably.

The errors can be even further reduced by increasing the ratio between the aperture of the mask and the beam area. Unfortunately, it is not possible to completely eliminate the error arising when a mask is used in the measurements. The wavelength-dependent interplay between the mask and sample will still prevail, since the ratio between the mask aperture and beam area can not be made arbitrarily large.

In order to obtain the most accurate reflectance values on small samples, the measurements should be performed obeying the following requirements. First, the mask must be combined with a properly focused sample beam. Secondly, the sample beam must be carefully adjusted in order to avoid any direct illumination of the mask. Third, the ratio between the mask aperture and the beam area should be chosen to be as large as possible.

Considering the transmittance measurements on small samples, it was found that the accuracy is in general much higher than the accuracy of the reflectance measurements. This is ascribed to the nature of the transmittance measurements, where the low transmittance of the mask ensures that only a small amount of the light illuminating the mask will enter the sphere directly. Despite this result, it was found that the mask alone introduces larger measuring errors than when the mask is combined with a properly aligned and focused sample beam. Additional experiments have been carried out on the test sample in an attempt to further improve the accuracy of the transmittance measurements. The sample was attached to the entrance port by means of two thin rigid supports, which were not illuminated. The result of these measurements is that a relative measuring error below 1% at all wavelengths can be obtained.

Measurements performed primarily on leaves from Hibiscus, rosa sinensis, show that the general conclusions made above are also valid for samples with a more inhomogeneous internal structure than the test sample. The errors will be of the same order of magnitude for the two kinds of samples, but the wavelength dependence will be different. It is therefore not

possible to determine a correction curve from the measurements on the test sample that can be used to correct the data obtained from an arbitrary sample.

ACKNOWLEDGMENT

We wish to thank Claus Vaarning for contributing to the postprocessing of the raw data.

1. A. Brunsting, R. S. Hernicz, and A. J. Dosmann, Appl. Opt. **23,** 4218 (1984).
2. G. Kortüm, *Reflectance Spectroscopy, Principles, Methods, Applications* (Springer Verlag, Berlin, 1969).
3. *Labsphere, A Guide to Reflectance Spectroscopy*.
4. *UV Winlab Software Guide* (Perkin Elmer, 1997).
5. *Acquisition of High Quality Transmission Spectra of Ultra-Small Samples,* www.perkinelmer.com (application note).
6. *Small Spot Kit for the 150 mm Integrating Sphere Reflectance Accessory,* www.perkinelmer.com.
7. N. Lobalzo and A. Voloboy, "Physically Based Lighting Model for Cloth and its Validation", Conference Proceedings 18th International Conference on Computer Graphics and Vision (Moscow State University, Moscow, Russia, June 23–27, 2008), pp. 61–68.